Explosivity of nanomaterials for lithium-ion battery electrodes

Sofia Ubaldi, Ghislain Binotto, Amandine Lecocq, Guy Marlair, Aurélie Aube, Arnaud Bordes, Paola Russo

Explosivity of nanomaterials for lithium-ion battery electrodes

Sofia Ubaldi [a], Ghislain Binotto [b], Amandine Lecocq [b], Guy Marlair [b], Aurélie Aube [b], Arnaud Bordes [b] & Paola Russo [a]

[a] Department of Chemical Engineering Materials Environment, Sapienza University of Rome, Rome, Italy
[b] INERIS, Verneuil-en-Halatte, France

E-mail: paola.russo@uniroma1.it

Abstract

As the European Union tries to develop important LIB production capacity by supporting the development of many gigafactories, new materials are under investigation to enhance the Lithium-ion batteries (LIBs) performances. A promising way onwards seems to be the optimization of the chemical composition of LIBs using nanomaterials (NMs). NMs most frequently used as active materials for the anode are silicon, lithium titanate oxide (LTO) and graphite. In addition, carbon black (CB) is used as an additive to increase the conductivity and the electrical performance of LIBs. Even if NMs are beneficial for LIB performances, the reduction of the particle size might induce an explosive behaviour of the powder used during manufacturing. For this reason, a study on crucial NMs safety was conducted to evaluate both physicochemical characteristics and relating explosivity risks of those NMs to ensure their safe production, handling and use, including in the gigafactories under construction all over Europe. Firstly, the characterization of the pristine NMs was performed (i.e., median particle size (d_{50}), and specific surface area (SSA)). Then, explosion parameters were assessed (i.e., minimum explosible concentration (MEC), maximum explosion pressure (P_{max}) and deflagration index (K_{st})) according to the standards. For LTO materials, no explosivity is observed due to the lack of combustibility and absence of any explosion-prone chemical group. A rise in the explosion's parameters was noted with the material's reduction in size from micro to nanoscale. In general, for the NMs, a smaller concentration of combustible dust mixed with air is needed for a deflagration to occur. This deflagration leads to higher maximum pressure values that in addition are set faster. For example, the micro-C exhibited no explosive behaviour, while the nano-C showed weak explosive severity (K_{max} = 63 bar m/s). Consequently, the utilisation of nanomaterials in the production of LIBs necessitates that the risk assessment be conducted with due consideration of the heightened explosion risk that is due to their use.

Keywords: *nanomaterials, NMs, Lithium-ion batteries, LIBs, explosion, P_{max}, $K_{st.}$*

Introduction

The available active powder materials for the anode and the cathode are limited by pore size and volume density. The current electrode active materials have micro-sized dimensions that limit the intrinsic diffusivity of the Li-ion intercalation in the solid state on the anode and that can pass through the separator. To enhance both the intercalation/deintercalation and the charge/discharge rates, the micro powders used as active materials can be substituted with either the same or different materials, thereby achieving nano-scale driven performance (Jiang, Hosono, and Zhou, 2006). Nanomaterials (NMs) have a smaller size, resulting in a shorter diffusion length and a higher contact area between active materials and electrolyte (Corcione and Frigione, 2012). This can enhance the performance and energy storage capacity of batteries while reducing their dimensions. Table 1 reports the different NMs currently under investigation for use as materials for the positive or negative electrode. NMs can take on various morphologies, including nanoparticles (NPs), nanotubes (NTs), nanowires (NW),

hollow nanosphere, and porous nanostructure. They can be used as pure materials, after mixing with other substances or as a coating for other materials.

***Table 1**. A summary of the NMs under investigation, with the relative application and reference*

Material	Application	Reference
Si	Anode	Wang et al., 2015
Si	Anode	Chen et al., 2012
Carbon coating on the Si surface	Anode	Wang et al., 2015
Core-shell amorphous silicon-carbon	Anode	Sourice et al., 2016
Mixing Si with C-based	Anode	Chen et al., 2012
Mixing Si with C-based	Anode	Chen et al., 2017
Si with polymer and chemical bonding	Anode	Erk et al., 2013
Si with polymer and chemical bonding	Anode	Assresahegn and Bélanger, 2017
Hybrid 0D and 1D Si	Anode	Pinilla et al., 2020
SiO_2	Anode	Al Ja'farawy et al., 2021
$Li_4Ti_5O_{12}$	Anode	Hudak, 2014
Carbon black (CB)	Anode additive	Hu, Zhong and Yan, 2021
$LiFePO_4$	Cathode	Hudak, 2014

Table 1 shows that the research in the field of the NMs is mainly focused on the anode materials. The two main possibilities for NMs as anode active material are titanium (Ti) (Hudak, 2014) and silicon (Si) (Eshetu et al., 2021). Additives, such as the carbon black, have also been evaluated for their ability to enable fast charging of batteries when added to the anode composition. The principal form is the $Li_4Ti_5O_4$, but various form of TiO_2 can also be used. The cycling mechanism of $Li_4Ti_5O_{12}$ is quite similar to that of $LiFePO_4$. The process relies on Li^+ insertion due to the formation of $Li_7Ti_5O_{12}$ at 1.55 V versus Li/Li^+ . This leads to a theoretical capacity of 175 mAh/g and a high degree of reversibility. Lithium titanate spinel is used in a nanocrystalline or nanoparticulate state to achieve a higher charging rate and extended cycle life compared to the same material in micro-size. In literature, most studies focus on developing materials made of or with Si, to replace graphite (C) powder as an innovative anode. Silicon nanoparticles (Si-NPs) are chosen due to their higher gravimetric and volumetric capacity, which surpasses that of all other elements currently considered or studied for this purpose (Qi et al., 2017). This results in lighter batteries being produced. Si-NPs are an attractive option due to their abundance, low cost, and high theoretical capacity of 3579 mAh g^{-1}. When reacting with lithium, they form the alloy Li_xSi, where $0 < x < 3.75$. However, Si-NPs have two significant drawbacks. Firstly, they undergo a volume change during lithiation and de-lithiation, expanding and contracting by about 300 % in volume. Secondly, they have an unstable solid electrolyte interphase (SEI) (Li et al., 2023). The significant quantity of lithium results in substantial structural changes, which are expressed in volume and can reach up to 300 %. This expansion in volume represents the primary drawback of silicon NMs, which leads to an irreversible loss of capacity due to the continuous SEI formation and a poor retention capacity due to the pulverization of the active material, Si-NPs (Sun et al., 2022). For this reason, Si is not considered as an active material alone but is often coupled with other species, such as Si-NPs. Si-NPs act as a coating for carbon particles, and the mixing of Si-NP with C-based NM help to reduce the pulverization of Si by improving its electronic conductivity and structural stability (Enotiadis et al., 2018). As a cathode, $LiFePO_4$ is one of the most developed NMs (Hudak 2014). The material has several advantages, including low ionic and electronic conductivity, high theoretical capacity for full de-lithiation (170 mAh/g), and a degree of reversibility (between $LiFePO_4$ and $FePO_4$) due to the cycling mechanism.

The performance achievement must be benchmarked against subsequent safety characteristics, particularly of explosivity behavior of the pristine NMs. While the explosivity behavior of micro-sized materials is well-known, this potential hazard must be re-evaluated for NMs due to the

significant change in particle size distribution (Johnston, Mansfield, and Smallwood, 2017). The reduction in particle size results in an increase in specific surface area (SSA), which increases sensitivity to explosions and significantly rises their severity (Bouillard, 2015). For a better understanding of how the sensitivity and explosion severity of powders vary with particle size distribution from the micro to the nano range, please refer to Assresahegn and Bélanger (2017).

Various parameters can be used to express the explosivity and severity of an explosion. These parameters can be evaluated by lab-scale standardized explosivity tests, such as the minimum explosible concentration (MEC), the maximum pressure (P_{max}) and the deflagration index (K_{st}). The MEC and the explosivity factors, P_{max} and K_{max}, can be evaluated by conducting experiments inside a 20-L sphere apparatus, according to ISO/IEC 80079-20-2. This test describes the test methods for combustible dust and the determination of the explosive characteristics of dust clouds according to EN 14034. Part 1 determines the maximum explosion pressure (P_{max}) of dust clouds; part 2 determines the maximum rate of explosion pressure rise ((dp/dt)max) of dust clouds; and part 3 determines the lower explosion limit (LEL) of dust clouds. The deflagration index *(*K_{st}), can be calculated from the cube-root law in Equation (1) (Bartknecht et al., 1989):

$$K_{st} = \left(\frac{dp}{dt}\right)_{max} * V^{1/3} \quad (1)$$

where V is the volume of the vessel (m^3), t is the time (s), and $\left(\frac{dp}{dt}\right)_{max}$ is the maximum rate of pressure rise (bar/s).

Equation (1) provides the size-normalized maximum rate of pressure rise for a constant-volume explosion. The severity of the explosion can be classified as follows: a value of 0 indicates no explosion, values between 1 and 200 indicate a weak explosion, values between 201 and 300 a strong explosion, and values higher than 300 indicate a very strong explosion.

Although MEC, P_{max}, and $(dp/dt)_{max}$ can be easily determined, it is important to note that they are strongly dependent on material characteristics, such as particle size or SSA (Khudhur, Ali, and Abdullah, 2021). Previous studies dating back a decade have shown an increase in the ignitability and explosivity of combustible powders when shifting from a micro to a nano particle size distribution (PSD) range (Dufaud et al., 2011). The MEC of the NP material is lower compared to the micro-scale material and is directly proportional to the bulk density. According to Dufaud et al. (2011), the explosion severity of Al powder tends to increase as the SSA decreases, before reaching a peak for 1 μm particle size. Therefore, the nanosized sample ignites at lower ignition energies and significantly lower dust amounts than is the micrometric sample.

The objective of this work is to assess the risk of explosivity associated with critical nanometric materials that are used to enhance the performance of the new LIBs. The comparison in this study includes both micro and nano sized materials to evaluate the change in explosivity properties between these particle size ranges. The materials selected for the study included Si, C, and LTO, which are under investigation for the anode of LIBs. Additionally, CB was selected as the main additive. The explosivity parameters were evaluated using the standard test, ISO/IEC 80079-20-2. Physical properties characterization was conducted for all selected materials to correlate explosivity-related parameters with their physical properties. These assessments can improve the safety assessment of dust explosions in process industries, including the gigafactories currently under construction throughout Europe (Eckhoff, 2003).

1. Materials and Methods

1.1. Materials

As a general rule in material selection, chemically similar materials were supplied at both micro and nanoscales. Dedicated use for the Li-ion battery field was a selection criterion, especially for NMs.

Regarding the micrometric reference materials, the selection process was less strict. Sometimes, the choice was not based solely on their proven use in batteries but also on the interest in accessing well-characterized micro powder materials for larger applications. For example, micro LTO ($Li_4Ti_5O_{12}$) for has a registration dossier available on the European Chemical Agency (ECHA) website.

The selection process concluded by gathering the following materials: the related PSD data extracted from the corresponding material safety data sheet (MSDS), as shown in Table 2.

***Table 2**. List of the materials considered in this work*

Materials	Purity (%) and PSD	Producer	References
Natural Graphite (C) Nanopowder/Nanoparticles	purity: 99.9 %, PSD: 400 nm - 1.2 µm	MTI Corporation	-
MesoCarbon MicroBeads (MCMB) graphite powder for Li-ion battery anode	purity: 99.96 % PSD: 8.087 µm – 33.080 µm	MTI Corporation	-
Lithium Titanate Oxide powder for Li-ion battery anode	purity: > 98 % PSD: 0.2 µm – 34 µm	MTI Corporation	-
Lithium Titanate Oxide	PSD: 2.26 µm	-	ECHA dossier (LTO, ECHA)
Carbon black Monarch 1300®	PSD: 13 nm	Cabot Corporation	Vignes et al., 2023
Carbon black	PSD: 17 µm	-	ECHA dossier (Carbon Black, ECHA)
Silicon powder	purity: 99+ % PSD: 50-100 nm	IolitecNanomaterials	Vignes et al., 2023
Silicon	PSD: 13.5 µm	-	ECHA dossier (Si, ECHA)

The physical and explosivity properties of both micro and nano materials have been characterized.

1.2. Methods

The explosivity behaviour is closely linked to the physical properties of selected powders. Therefore, a first characterization of materials was performed at both micro and nano levels to correlate the obtained data in our work.

1.2.1. Characterization of the pristine materials

The main characteristics to be evaluated for the pristine NMs are PSD, SSA and the density. For all these measurements, there are standards that can be applied to unify the data obtained.

The particle size distribution measurements were evaluated according to ISO 13320 (ISO, 2020). The tests were performed with a HELOS-KR instrument equipped with Quixel or Rodos dispersing units (Sympatec). For the analysis, the test material was first dispersed in a solution of water and octylphenoxypolyethoxyethanol, a non-denaturing detergent (IGEPAL®, Merck), and further shaken at ultrasonic frequency of 40 kHz, to maximize dispersion. The SSA of porous solids was measured by physical adsorption of nitrogen gas according to the Brunauer, Emmett and Teller (BET) method, following ISO 9277 (ISO, 2010). The SSA tests were performed with a 3-Flex (Micromeritics) instrument. Finally, the (skeletal) density was evaluated with helium gas according to ISO 12154:2014. Density tests were performed using an Accupyc II 1340 (Micromeritics).

1.2.2. Explosivity of the materials

The parameters that define the explosivity severity of a material are MEC, P_{max}, K_{st}. These parameters have to be evaluated from specific tests according to the ISO/IEC 80079-20-2 (ISO, 2016). The tests were performed inside a 20-L sphere (Kuhner), where the ignition source, placed in the center of the sphere, triggers an energy of 10 kJ for the evaluation of P_{max}, K_{st} or 2 kJ for the determination of MEC.

2. Results and discussion

The physical properties and explosivity hazards of the materials, both at the micro and nanoscale levels, have been evaluated using the same standard procedures in order to highlight any significant differences induced by the three orders of magnitude change in size studied.

2.1. Characterization of the pristine materials

A multi-criteria physical characterization of the pristine materials was carried out, even if some information was already available in the MSDS, in order to confirm the reported values. The PSD can be qualified according to various size-related parameters related to number, weight or surface based criteria. d_{50}, which reflects the median particle size distribution (50% of the total particles are smaller and 50 % are larger) was primarily used here for comparison.

The results for the nano-graphite (nano-C) are reported and discussed here in detail, while the results for the other materials are summarised in Table 3. In particular, the PSD curve for the nano-C is shown in Figure 1.

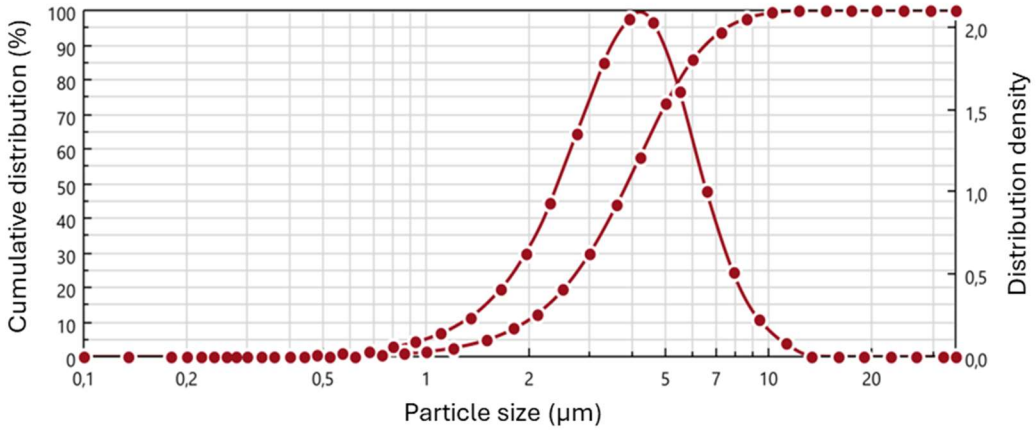

Fig. 1. *Size distribution curve of the nano-C*

The distribution appears to be monodispersed, centered around the value of 4 µm, close to the d_{50} value (3.86 µm). From the cumulative distribution curve, the so called d_{10} and d_{90} parameters, which fix 10 % and 90 % of the cumulative particle size distribution in the test powder, can be easily determined as 1.94 µm and 6.63 µm, respectively. Corresponding data can then further be used to qualify the particle size metric range more globally. The values indicate that the supplied "nano-C" nanomaterial appears to be in the micrometric particle range, in contrast to the data given in the relevant MSDS issued by the manufacturer. This is indicated by the fact that more than 50% of the particles have a size greater than the 1-100 nm range indicated by the European Commission. In fact, the European Commission has standardized the terms in the 10th Commission Recommendation of June 2022: this text defines that *Nanomaterials means solid particles where 50 % or more of the particles in the number-based size distribution of one or more external dimensions are in the size range 1 nm to 100 nm* (European Commission, 2020).

This ambiguity in the interpretation of results is due to the extrinsic properties of NMs, which tend to agglomerate, especially when dispersed in solution, such as IGEPAL®, resulting in larger agglomerates. In order to reduce the ambiguity in the classification of the NMs a new parameter can be mathematically evaluated, which is the volume specific surface area (VSSA). This parameter is obtained by the combination of two physical parameters, the density and the SSA of the materials. The VSSA, expressed in m^2/cm^3, can be calculated according to Equation (2) (Dazon et al., 2020):

$$VSSA = SSA * \rho \quad (2)$$

where SSA is the specific surface area (expressed in m^2/cm^3) and ρ is the density (expressed in g/cm^3).

If the result of Equation (2) is higher than 6 m^2/cm^3, the material under investigation can be considered as a nanoscale material (CEU, 2019). Therefore, this parameter can be used as an alternative method to assess whether the material is a nanomaterial or not (Bau et al., 2021).

For the NM under investigation the ρ is equal to 2.4 g/cm^3, while the SSA is equal to 9.7 m^2/g. So, applying the Equation (2), the VSSA for the nano-C under investigation is 23.3 m^2/cm^3, which is higher than the limit of 6 m^2/cm^3. The materials can therefore be defined as NMs, although the PSD curve would suggest a different interpretation.

Physical profiles of the other materials of interest in the research are summarized in Table 3.

***Table 3**. Physical properties of various micro- and nanoscale materials, either collected from related MSDS or obtained experimentally*

Material	PSD from MSDS	Size (d_{50})	ρ (g/cm^3)	SSA (m^2/g)	VSSA (m^2/cm^3)
Micro-CB	n.a.	17 µm	n.a.	n.a.	n.a.
Nano-CB	n.r.	13 nm	n.r.	377	n.r.
Micro-C	1.07 µm – 60.26 µm	17.79 µm	2.3	0.7	1.7
Nano-C	400 nm- 1.2 µm	3.86 µm	2.4	9.7	23.3
Micro-LTO	n.a.	2.46 µm	n.a.	n.a.	n.a.
Nano-LTO	200 nm – 34 µm	1.13 µm	3.6	4.6	16.6
Micro-Si	n.r.	13.5 µm	n.r.	1.3	n.r.
Nano-Si	50 nm – 100 nm	-	0.36	18.6	6.7

n.a.: data not available from ECHA web site. n.r.: not reported.

From the data presented in Table 3, there are some difficulties in making a detailed comparison of the granulometry ranges of the two selected sets of materials (micro and nano), either obtained from MSDS or reflected by their d_{50} as measured in our work. Again, this may be because the powders and the relative dusts of NMs may be difficult to fully disperse into primary particles, leading to the particles behaving as if they were coarser. This could results in a higher measured d_{50} values than those intrinsically associated with an ideal dispersion of corresponding NPs. However, this issue can be resolved by basing the identification of the metric range of the test materials on the VSSA parameter, as explained above for nano-C. This alternative method, appears to eliminate inconsistencies in the classification of test materials within the micro or nano range, according to their respective MSDS. For example, both graphite materials have a d_{50} of micro (17.79 µm for micro-C and a lower value of 3.86 µm for nano-C), the results still leave some doubts as to whether nano-C is a true nanomaterial. Nevertheless, a comparison of the VSSA values provides a more distinct differentiation between these materials. In fact, the VSSA for micro-C is equal to 1.7 m^2/cm^3 while the VSSA for nano-C is equal to 23.3 m^2/cm^3. In other words, the first VSSA value is well below 6 m^2/cm^3, while the second VSSA value is well above 6 m^2/cm^3. This confirms the nano range in the second case and micro range in the first one, in accordance with the material designation. Similarly, the value of VSSA calculated for the nano-LTO and e nano-Si confirms their classification as NMs.

From previous results it can be concluded that analytical techniques, specifically laser diffraction, can be used to evaluate the particle size distribution, but it is not necessarily an adequate technique for the nanometric range of PSD, especially since it has not been developed specifically/exclusively for this range of particles. It can certainly give a general trend, but the results needs to be confirmed by e.g. dynamic light scattering (DLS) or transmission electron microscopy (TEM). Indeed, if the particles are not fully dispersed, the results obtained may be somewhat biased by particle agglomeration, depending on the particle morphology. For instance, cylindrical morphology may lead to interpretation problems. Therefore, it can be concluded that at the moment the mathematical evaluation by VSSA is the most effective technique to confirm the nano-size dimension of the materials, as defined in the NanoDefine project (Mech et al., 2020). An unique classification method of the NMs must be drawn up in order to obtain a uniform classification.

These assessments are of fundamental importance for the correct characterisation of the materials during the production steps, such as quality control. Thay are also of great significance in terms of safet, as they enable the assessment of the risk of explosivity.

2.2. Explosivity of the pristine materials

The explosivity tests were carried out according to the relative standard procedures on all the pristine materials, however only the results for the nano-C are reported in detail, while for the other materials the results are reported in Table 4. The key parameters that qualify the sensitivity and severity of a potential ATEX generated by the nano-C, are shown in Figure 2.

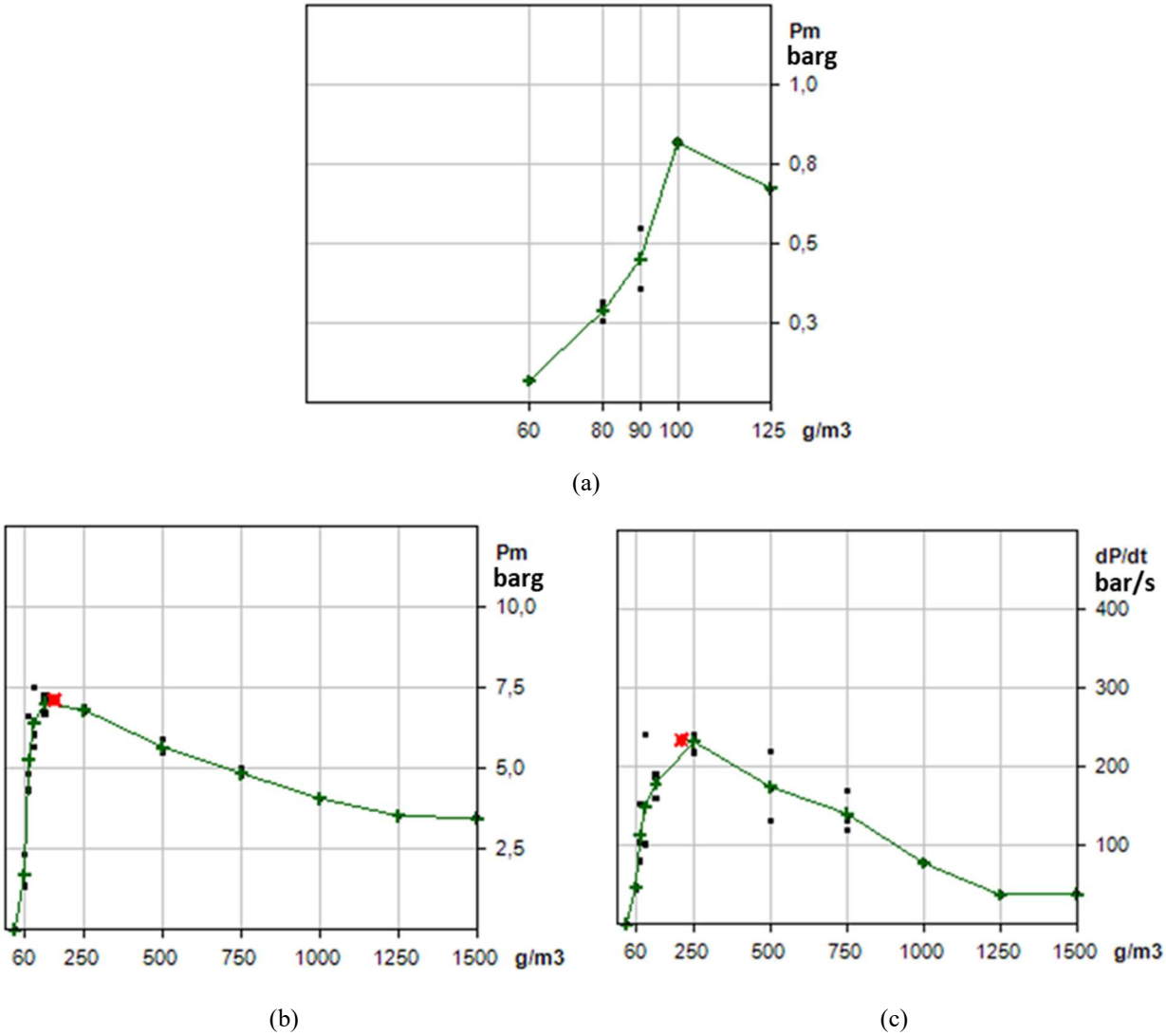

Fig. 2. *Graphs of the explosivity parameters of nano-C: (a) MEC, (b) P_{max}, (c) $(dp/dt)_{max}$*

From Figure 2a it is possible to determine the MEC, which for the nano-C is equal to 80 g/m^3. This result indicates that is from this value of concentration the nano-C can generate an ATEX. In fact, by examining the profile over the whole concentration range (Figure 2b), P_{max} is found to be of the order of 7.1 barg. The maximum rate of explosion pressure rise $(dp/dt)_{max}$ of nano-C dust is found to be around 234 ± 47 bar/s (Figure 2c). From this last parameter the explosivity severity can be quantified according to Equation (1) and by the associated criteria. The resulting K_{st} is 63 ± 13 bar m/s which corresponds to a weak explosion.

The same parameters for the other materials at different size ranges are reported in Table 4.

***Table 4**. Explosivity parameters for the various micro- and nanoscale materials*

Material	MEC (g/m^3)	P_{max} (barg)	$\left(\frac{dp}{dt}\right)_{max}$ (bar/s)	K_{st} (bar m/s)	Explosivity severity
Micro-CB	125	3	n.a.	6	Weak
Nano-CB	70	7.8	337	91	Weak
Micro-C	0	*	*	*	Nil
Nano-C	80	7.1	234	63	Weak
Micro-LTO	n.a.	n.a.	n.a.	n.a.	n.a.
Nano-LTO	0	*	*	*	Nil
Micro-Si	n.r.	7.8	170	46	Weak
Nano-Si	135	7.9	249	68	Weak

*n.a.: not available in the ECHA dossier. n.r.: not reported. *: not conducted, due to the MEC = 0.*

From a first comparison of the data presented in Table 4 reveals a consistent trend across the parameters, with the exception of LTO. It can be observed that downscaling the PSD of the materials, from micro to nano, results in an increase in the sensitivity or severity of the explosion. Specifically, the MEC value decreases with decreasing dimensions, while for P_{max} and $K_{st,}$ an increase in these parameters occurs when the dimensions of the materials decrease. In general, therefore, for NMs, a lower concentration of dust is required for a deflagration to potentially occur, and this deflagration leads to higher pressure values and faster rate of pressure rise. Finally, the evaluation of the explosivity severity resulting from the application of Equation (1) and the associated criteria is given in Table 4.

The most significant difference in terms of explosivity parameters is obtained by comparing the micro-C and nano-C materials. In fact, the micro-C dispersed inside the 20-L sphere does not generate an ATEX (MEC = 0 g/m^3), whereas the nano-C material can cause an explosion at a concentration at least equal to the MEC value (80 g/m^3). The other explosivity parameters, i.e., $(dp/dt)_{max}$ and P_{max}, for the micro-C were not available due to the non-explosivity of the materials. So, the explosivity severity of the micro-C can be classified as nil (K_{st} = 0 bar m/s), while that of nano-C is classified as weak.

Both Si and CB also exhibit , albeit to a lesser extent than C, an increase in explosivity behavior as the particle size range shifts from micro to nano. With regard to CB, the MEC obtained passes from 125 g/m^3 for the micro-CB to 70 g/m^3 for the nano-CB, representing a reduction of one order of magnitude. In any casee, the difference in the P_{max} obtained for the two sizes is not significantly different (3 barg for micro-CB vs 7.8 barg for nano-CB). The resulting K_{st} values for both dimensions are included in the range between 1 and 200 bar m/s, indicating that the explosivity severity of micro and nano CB is classified as weak.

In the case of Si, the differences between the various explosiveness parameters are not significantly different, which lead to the same final classification. Consequently, both Si materials lead to a weak explosion. Thus, for the Si and the CB, the transition from the micro to the nanoscale shows a decrease in MEC, but since K_{st} remains in the same order of magnitude on both metric scales, i.e. less than 100 ·bar m/s, a weak explosion severity is both cases.

Finally, the comparison between the micro-LTO and the nano-LTO remains complex due to lack of data for the micro material (no data available on the ECHA website for this material). As regards the LTO material, the explosion risk is indeed practically non-existent, whatever the PSD. The explanation lies in two facts: according to the chemical formula of LTO, the material does not have any significant combustibility property, thus suppressing any dust explosion hazard. In addition, this material does not contain any explosion-prone chemical group, which therefore cannot explode per se. A similar trend has been observed for the nano-LTO, which, when dispersed in air, does not generate an explosive atmosphere as the MEC is zero and even the ignition temperature is higher than 1000 °C indicating the thermal stability of the LTO material.

These assessments are of great importance for the increased awareness of the explosion risk of powders used in process industries, such as the gigafactories under construction around the world and in Europe. Conventional processing for the production of a lithium-ion cell consists of three steps: (1) electrode production, (2) cell assembly, and (3) cell formation (Örüm Aydin et al., 2023). The phase that is most affected by the variation of the material size and its relative explosivity is that of the electrode production. In fact, in this phase, the different pure powders of the active material and the conductive agent, previously dosed, are placed inside the mixer and added to the electrode slurry, the so-called binding solution. Subsequently, the mixture is degassed and then pumped out so as to obtain a uniform, homogenous coating over the current collector. Finally, several drying steps are conducted in the oven. The proposed procedure is general, as each manufacturer then applies different operating conditions and/or different treatments. In any case, the transition from micro-materials to NM requires an update of the technical procedure and/or instruments used. In particular, the tools used during the mixing of pure NMs must be adapted to the pressure and must avoid the generation of an ATEX atmosphere within the plant at any stage of the process.

3. Conclusions

On the anode side, to improve the performance of LIBs, nano-Si, nano-LTO and nano-C are the most studied active materials, while nano-CB can be used as additive to enhance the conductivity. The increase in the performance is accompanied by a potential increase in explosivity risk during the manufacturing phases, which is strongly correlated with the decrease in particle size.

Firstly, a characterization of the materials, both at micro and nano size, was carried out to obtain more detailed information on the granulometry of the particle in the powder, i.e., d_{50}. Anyway, in the case of NMs the evaluation of this parameter can be affected by an error, since the powders and relative dusts of NMs can be difficult to disperse completely into primary particles and therefore behave as coarser particles. So, the classical analytical technique, such as laser diffraction, needs additional confirmation by DLS or TEM. An alternative mathematically method, based on the determination of the VSSA, has been developed to observe the real differences in the PSD of the materials and to confirm the classification of selected materials as NMs (VSSA > 6 m^2/cm^3). By this mathematically method the ambiguity between the experimental data and the data given in the relevant MSDS issued by the manufacturer were solved.

In terms of explosion risk, the key parameters, i.e., MEC, P_{max} and K_{st}, were evaluated according to the relevant standard procedures. By reducing the size of the material, from micro- to nano-size, an increase in explosion severity for all the NMs, except for LTO, was observed. This behaviour is increasingly evident from nano-CB to nano-Si up to the extreme case of nano-C. In fact, regarding the graphite, the micro-C does not show any explosive behaviour (MEC = 0 g/m^3) while the nano-C shows a weak explosive severity (K_{st}=63 bar m/s) associated to a MEC of 80 g/m^3. Finally, both nano and micro LTO showed zero risk of explosion due to the non-combustible nature of the material. In conclusion, the increase in the risk of explosivity, due to the size reduction, is confirmed in terms of sensitivity and severity of explosion by the determination of the explosivity parameters.

These assessments are fundamental both for a correct characterization of the materials during the production and assembly phase of the cells and for a greater awareness of the risk of explosion of the NMs used in the process industries such as the gigafactories under construction all over the world as in Europe.

A future application of this work could be to consider not only the pristine single materials but also the coupled NMs, such as Si and CB together in the same formation ratio used in the Li-ion cell anode. In fact, the anode will not consist of a single NM, but of the coupling of two or more NMs and additives to achieve the best possible performance.

Acknowledgements

The study received funding from the SAF€RA 2022 joint call for proposals in the year 2022 for the project entitled "Safety evaluation of nanomaterials in Novel EES materials and LIBs (Nano-SaNE)".

References

Al Ja'farawy, M.S., Hikmah, D.N., Riyadi, U., Purwanto, A. & Widiyandari, H. (2021). A Review: The Development of SiO2/C Anode Materials for Lithium-Ion Batteries. *Journal of Electronic Materials,* 50(12): 6667–87.

Assresahegn, B.D. & Bélanger, D. (2017). Synthesis of Binder-like Molecules Covalently Linked to Silicon Nanoparticles and Application as Anode Material for Lithium-Ion Batteries without the Use of Electrolyte Additives. *Journal of Power Sources,* 345: 190–201.

ASTM. 2022. "ASTM B923-22 Standard Test Method for Metal Powder Skeletal Density by Helium or Nitrogen Pycnometry." https://www.astm.org/b0923-22.html.

Bartknecht, W., Bartknecht, W. & Bartknecht, W. (1989). *Dust Explosions: Course, Prevention, Protection*. Berlin Heidelberg: Springer.

Bau, S., Dazon, C., Rastoix, O. & Bardin-Monnier, N. (2021). Effect of constituent particle polydispersion on VSSA-based equivalent particle diameter: Theoretical rationale and application to a set of eight powders with constituent particle median diameters ranging from 9 to 130 nm. *Advanced Powder Technology*, 32(5): 1369–1379.

Bouillard, J.X. (2015). Fire and Explosion of Nanopowders. In *Nanoengineering*, 111–48. Elsevier.

Chen, S., Gordin, M.L., Yi, R., Howlett, G., Sohn, H. & Wang, D. (2012). Silicon core–hollow carbon shell nanocomposites with tunable buffer voids for high capacity anodes of lithium-ion batteries. *Physical Chemistry Chemical Physics*, 14(37): 12741.

Chen, S., Shen, L., Van Aken, P.A., Maier, J. & Yu, Y. (2017). Dual-Functionalized Double Carbon Shells Coated Silicon Nanoparticles for High Performance Lithium-Ion Batteries. *Advanced Materials,* 29(21): 1605650.

CEU. (2019). Identification of nanomaterials through measurements :points to consider in the assessment of particulate materials according to the European Commission's Recommendation on a definition of nanomaterial. *Joint Research Centre*, LU: Publications Office. Available online: https://data.europa.eu/doi/10.2760/7644

Chen, S., Gordin, M.L., Yi, R., Howlett, G., Sohn, H. & Wang, D. (2012). Silicon Core–Hollow Carbon Shell Nanocomposites with Tunable Buffer Voids for High Capacity Anodes of Lithium-Ion Batteries. *Physical Chemistry Chemical Physics,* 14(37): 12741.

Corcione, C. & Frigione, M. (2012). Characterization of Nanocomposites by Thermal Analysis. *Materials*, 5(12): 2960–80.

Dazon, C., Fierro, V., Celzard, A. & Witschger, O. (2020). Identification of Nanomaterials by the Volume Specific Surface Area (VSSA) Criterion: Application to Powder Mixes. *Nanoscale Advances,* 2(10): 4908–17.

Dufaud, O., Vignes, A., Henry, F., Perrin, L. & Bouillard, J. (2011). Ignition and Explosion of Nanopowders: Something New under the Dust. *Journal of Physics: Conference Series,* 304: 012076.

ECHA. Carbon Black: Echa Dossier. Available online: https://echa.europa.eu/ro/registration-dossier/-/registered-dossier/16056/1/1. (Accessed on March 4, 2023).

ECHA. LTO: ECHA dossier. Available online: https://echa.europa.eu/ro/registration-dossier/-/registered-dossier/5366/1/1. (Accessed March 4, 2023).

Eckhoff, R.K. (2003). *Dust Explosions in the Process Industries*. 3rd. ed. Amsterdam: Gulf professional publ.

Enotiadis, A., Fernandes, N.J., Becerra, M.A., Zammarano, M. & Giannelis, E.P. (2018). Nanocomposite Electrolytes for Lithium Batteries with Reduced Flammability. *Electrochimica Acta,* 269: 76–82.

Erk, C., Brezesinski, T., Sommer, H., Schneider, R. & Janek, J. (2013). Toward Silicon Anodes for Next-Generation Lithium Ion Batteries: A Comparative Performance Study of Various Polymer Binders and Silicon Nanopowders. *ACS Applied Materials & Interfaces,* 5(15): 7299–7307.
Eshetu, G.G., Zhang, H., judez, X., Adenusi, H., Armand, M., Passerini, S. & Figgemeier, E. (2021). *Nature Communications*, 12(1).
European Commission. (2020). The NanoDefine methods manual. *Joint Research Centre,* LU: Publications Office, 2020. Available online: https://data.europa.eu/doi/10.2760/79490
European Standard (EN) (2011). BS EN 14034-3:2006+A1:2011 Determination of Explosion Characteristics of Dust Clouds Determination of the Lower Explosion Limit LEL of Dust Clouds. Available online: https://www.en-standard.eu/bs-en-14034-3-2006-a1-2011-determination-of-explosion-characteristics-of-dust-clouds-determination-of-the-lower-explosion-limit-lel-of-dust-clouds/.
Hu, J., Zhing, S. & Yan, T. (2021) Using carbon black to facilitate fast charging in lithium-ion batteries. *Journal of Power Sources*, 508(230342).
Hudak, N.S. 2014. Nanostructured Electrode Materials for Lithium-Ion Batteries. *Lithium-Ion Batteries*, 57–82. Elsevier. https://doi.org/10.1016/B978-0-444-59513-3.00004-2.
Iolitec Nanomaterials. Silicon NM-0020-HP. Available online: https://nanomaterials.iolitec.de/index.php/en/products/metals/NM-0020-HP. (Accessed February 13, 2024)
ISO (2010). ISO 9277:2010 Determination of the Specific Surface Area of Solids by Gas Adsorption — BET Method. Available online: https://www.iso.org/standard/44941.html.
ISO (2016). ISO/IEC 80079-20-2:2016 Explosive Atmospheres — Part 20-2: Material Characteristics — Combustible Dusts Test Methods. Available online: https://www.iso.org/standard/66564.html.
ISO (2020). ISO 13320:2020 Particle Size Analysis — Laser Diffraction Methods. Available online: https://www.iso.org/standard/69111.html.
Jiang, C., Hosono, E. & Zhou, H. (2006). Nanomaterials for Lithium Ion Batteries. *Nano Today,* 1(4): 28–33.
Johnston, L., Mansfield, E. & Smallwood, G.J. (2017). Physicochemical Properties of Engineered Nanomaterials. In *Metrology and Standardization of Nanotechnology*, edited by Elisabeth Mansfield, E., Kaiser, D.L., Fujita, D. & Van De Voorde, M. 99–114. Weinheim, Germany: Wiley-VCH Verlag GmbH & Co. KGaA.
Li, Y., Li, Q., Chai., J., Wang, Y., Du, J., Chen, Z., Rui, Y., Jiang, L. & Tang, B. (2023). Si-based Anode Lithium-Ion Batteries: A Comprehensive Review of Recent Progress. *ACS Materials Letters*, 5(11): 2948-2970.
Khudhur, D.A., Ali, M.W., & Tuan Abdullah, T.A. (2021). Mechanisms, Severity and Ignitability Factors, Explosibility Testing Method, Explosion Severity Characteristics, and Damage Control for Dust Explosion: A Concise Review. *Journal of Physics: Conference Series,* 1892 (1): 012023.
Mech, A., Rauscher, H., Babick, F., Hodoroaba, V., Ghanem, A., Wohlleben, W., Hans, Marvin, Weigel, S., Brungel, R., Friedrich, C.M., Kirsten, Rasmussen, Loeschner, K. & Gilliland, D. (2020). The NanoDefine Methods Manual. Available online: https://publications.jrc.ec.europa.eu/repository/handle/JRC117501. (Accessed May 10, 2024).
MTI Corporation. Li4Ti5O12 Powder for Li-Ion Battery Anode, 200g/Bag - EQ-Lib-LTO. Available online: https://www.mtixtl.com/Li4Ti5O12PowderforLi-ionbatteryanode200g/bag-EQ-Lib-LTO.aspx. (Accessed July 19, 2023).
MTI Corporation. MCMB (MesoCarbon MicroBeads) Graphite Powder for Li-Ion Battery Anode, 250g/Bag - EQ-Lib-MCMB. Available online: https://www.mtixtl.com/MCMBMesoCarbonMicroBeadsGraphitePowderforLi-ionBatteryAnode250g.aspx. (Accessed July 19, 2023).
Nanographenex. Natural Graphite (C) Nanopowder/Nanoparticles, Purity: 99.9% Size: 400 Nm-1.2 Um. Available online: https://nanographenex.com/natural-graphite-c-nanopowder-nanoparticles-

purity-99.9-size-400-nm-1.2-um-nanoparticles?search=carbon&description=true&category_id=60&sub_category=true. (Accessed July 19, 2023).
Örüm Aydin, A., Zajonz, F., Günther, T., Dermenci, K., Berecibar, M. & Urrutia, L. (2023). Lithium-Ion Battery Manufacturing: Industrial View on Processing Challenges, Possible Solutions and Recent Advances. *Batteries,* 9(11): 555.
Pinilla, S., Park, S.-H., Fontanez, K., Márquez, F., Nicolosi, V. & Morant, C. (2020). 0D-1D Hybrid Silicon Nanocomposite as Lithium-Ion Batteries Anodes. *Nanomaterials,* 10(3): 515.
Qi, W., Shapter, J.G., Wu, Q., Yin, T., Gao, G. & Cui, D. (2017). Nanostructured Anode Materials for Lithium-Ion Batteries: Principle, Recent Progress and Future Perspectives. *Journal of Materials Chemistry A,* 5(37): 19521–40.
Sourice, J., Bordes, A., Boulineau, A., Alper, J.P., Franger, S., Quinsac, A., Habert, A., Leconte, Y., De Vito, E., Porcher, W., Reynaud, C., Herlin-Boime, N. & Haon, C. (2016). *Journal of power Sources*, 328: 527-535.
Sun, L., Liu, Y., Shao, R., Wu, J., Jiang, R. & Jin, Z. (2022). Recent Progress and Future Perspective on Practical Silicon Anode-Based Lithium Ion Batteries. *Energy Storage Materials,* 46:482–502.
Vignes, A., Dutouquet, C., Aube, A., Laurent, M., Bressot, C., Bouillard, J., Pohl, A., Ribalta, C. & Fonseca, S. (2023). Draft of the operational methodology for the use of dustiness for risk assessment of NMs and HARNs explosion risk in industrial scenario to support ATEX safety assessment, Deliverable D1.15, NanoHarmony H2020 EU Project, Grant agreement ID: 885931. Available online: https://ec.europa.eu/research/participants/documents/downloadPublic?documentIds=080166e505fe1678&appId=PPGMS.
Wang, L., Gao, B., Peng, C., Peng, X., Fu, J., Chu, P.K. & Huo, K. (2015). Bamboo Leaves Derived Ultrafine Si Nanoparticles and Si/C Nanocomposites for High-Performance Li-Ion Battery Anodes. *Nanoscale,* 7(33): 13840-13847.